Greetham, Gregory M. and Donaldson, Paul M. and Nation, Charlie and Sazanovich, Igor V. and Clark, Ian P. and Shaw, Daniel J. and Parker, Anthony W. and Towrie, Michael (2016) A 100 kHz time-resolved multiple-probe femtosecond to second infrared absorption spectrometer. Applied Spectroscopy, 70 (4). pp. 645-653. ISSN 0003-7028 , http://dx.doi.org/10.1177/0003702816631302

A 100 kHz Time-Resolved Multiple-Probe Femtoseconds to Second IR Absorption Spectrometer

G. M. Greetham[1], P. M. Donaldson[1], C. Nation[1], I. V. Sazanovich[1], I. P. Clark[1], D. J. Shaw[1, 2], A. W. Parker[1] and M. Towrie[1]*

1. Central Laser Facility, Science and Technology Facilities Council, Research Complex at Harwell, Rutherford Appleton Laboratory, Didcot, Oxfordshire, OX11 0QX, United Kingdom..

2. Department of Physics, University of Strathclyde, SUPA, 107 Rottenrow East, Glasgow, G4 0NG, United Kingdom.

** Corresponding author.*

Abstract

We present a dual-amplifier laser system for time-resolved multiple-probe IR spectroscopy based on the Yb:KGW laser medium. Comparisons are made between the ytterbium-based technology and titanium sapphire laser systems for time-resolved IR spectroscopy measurements. The 100 kHz probing system provides new capability in time-resolved multiple-probe experiments, as more information is obtained from samples in a single experiment through multiple-probing. This method uses the high repetition-rate probe pulses to repeatedly measure spectra at 10 μs intervals following excitation allowing extended timescales to be measured routinely along with ultrafast data. Results are presented showing

the measurement of molecular dynamics over > 10 orders of magnitude in timescale, out to 20 ms, with an experimental time response of < 200 fs. The power of multiple-probing is explored through principal component analysis of repeating probe measurements as a novel method for removing noise and measurement artefacts.

Index Headings

ULTRAFAST; TIME-RESOLVED; MID-INFRARED; MID-IR; LASER; SPECTROSCOPY; MULTIPLE-PROBING.

Introduction

Chemical and biological molecular changes occur over a wide range of timescales. Recent developments in our laboratory have extended ultrafast femtosecond optical delay measurements to nanoseconds and milliseconds by seeding dual-amplifiers with subsequent oscillator seed pulses (60 MHz oscillator corresponding to 14 ns steps) and multiple-probing with a high repetition rate probe (10 kHz probe measures spectra of change every 100 μs following excitation)[1]. Having demonstrated the potential of this approach, in chemistry[2, 3] and biology, particularly for measuring time-resolved IR (TRIR) spectra of light-activated protein dynamics[4-10], here we extend the technique using a higher repetition rate probe system (100 kHz, probing dynamics every 10 μs), providing an order of magnitude increase in information per experiment, compared to our previous work.

The 100 kHz laser system described in this paper is based on ytterbium potassium gadolinium tungstate (Yb:KGW) ultrafast amplifier technology[11], rather than the more commonly used (in ultrafast time-resolved measurements) titanium sapphire (Ti:S) lasers. The development

rate of ytterbium-based lasers at very high repetition rates has recently overtaken that of Ti:S systems, due to the better efficiency, with lower quantum defect and direct diode pumping of the laser medium (rather than high power Nd:YAG/YLF green laser pumping of Ti:S to generate 800 nm output). This efficient technology has found applications in laser machining and surgery fields, enhancing the development rate and improving reliability. The ability to drive optical parametric amplifiers (OPA) means that this industrial-quality technology can also be applied in scientific laboratories[12]. To our knowledge, this work is the first application of this technology to TRIR spectroscopy. One clear drawback of the ytterbium-based ultrafast lasers is their narrower spectral bandwidth relative to Ti:S, providing > 180 fs pulses, rather than the shorter pulses, > 30 fs, from a Ti:S system. Broader bandwidth and shorter pulse duration provide considerable advantages to time-resolved spectroscopy, enabling the probing of more spectral features in a single pulse and the measurement of very fast processes (< 100 fs). Increased bandwidth and pulse shortening can be obtained in OPA devices (providing ~ 100 fs pulses) and it is possible to pump non-collinear OPA (NOPA) systems with this technology to provide much shorter pulse lengths (< 7 fs) with outputs around 800 nm[13] and up to 4 μm with subsequent difference frequency mixing with narrowband fundamental in the near-IR[14]. Unfortunately, extension of NOPA schemes to generate stable, short, broadband mid-IR, > 4 μm, are currently limited due to materials and efficiency. The longer pulse durations (200 fs time-resolution limit is demonstrated below) still permit wide application to structural dynamics in chemistry and biology. The loss in bandwidth does limit spectral coverage in the IR probe of TRIR measurements, > 200 cm^{-1} compared with > 400 cm^{-1} usable bandwidth in Ti:S systems. In the present system, we reduce the impact of this bandwidth issue and gain advantage by using two independent probe OPAs to maximise the wavelength regions we are able to probe in a single measurement.

This paper describes the time-resolved multiple-probe spectroscopy (TRMPS) capability of the 100 kHz Yb:KGW system. Output characteristics such as spectral bandwidth, sub-picosecond temporal resolution and signal to noise capabilities are presented. We demonstrate the effectiveness of our approach through TRMPS measurements of tungsten hexacarbonyl ($W(CO)_6$) photo-dissociation across the picosecond – millisecond timescale and showing TRIR spectra of other samples over multiple spectral regions and at various repetition rates.

Principal component analysis and similar methods are often used to extract spectral information from complex data. Here we apply the method to identify noise and artefacts on the unique kinetic information available with the TRMPS method.

Experimental

The time-resolved multiple-probe IR spectrometer comprises a dual-amplifier ultrafast laser, optical parametric amplifiers, pump-probe sampling and IR spectrometers, see fig. 1. The principle of the experiment has been discussed previously[1], so details below are minimised to focus on the different technologies used and the significant advances made.

Compared to a single amplifier, the dual-amplifier system allows pump probe delays to go beyond the typical fs – ns range[15]. Using a single oscillator, the two amplifiers are seeded by the same or different seed pulses from the 80 MHz pulse train, allowing pump – probe delays to be stepped by 12 ns. Additionally, the two amplifiers can be individually optimised to provide dedicated outputs for pumping (higher energy, lower repetition rate) or probing (lower energy, higher repetition rate and higher bandwidth). The pump amplifier (**A**) provides 1030 nm, 100 kHz, 15 W, 260 fs output (Light Conversion Ltd, Pharos). The repetition rate

of this amplifier can be divided down programmatically by an internal pulse picker to pump repetition rates < 100 kHz allowing pump on – pump off difference measurements or the arbitrary probe : pump ratios in pump – probe – probe – probe (TRMPS) experiments. The probe amplifier (**B**) provides 1030 nm, 100 kHz, 6 W, 180 fs output (Pharos SP).

Amplifier **A** drives a single BBO-based 515 nm pumped OPA (Light Conversion Ltd, Orpheus HP) to provide outputs spanning 210 – 2600 nm (including signal and idler harmonics), which are typically used as pump pulses in electronic excitation experiments. Subsequent difference frequency generation (DFG) processes in KTA and GaSe provide mid-IR output in the range of 2100 – 13000 nm (used as pump pulses in vibrational excitation experiments, such as 2D-IR spectroscopy, to be discussed in a subsequent paper).

Amplifier **B** drives two 3 W BBO/KTA-based OPAs (Light Conversion Ltd, Orpheus ONE) to provide outputs spanning 1350 – 4800 nm. DFG in GaSe provides outputs in the range of 4000 – 13000 nm.

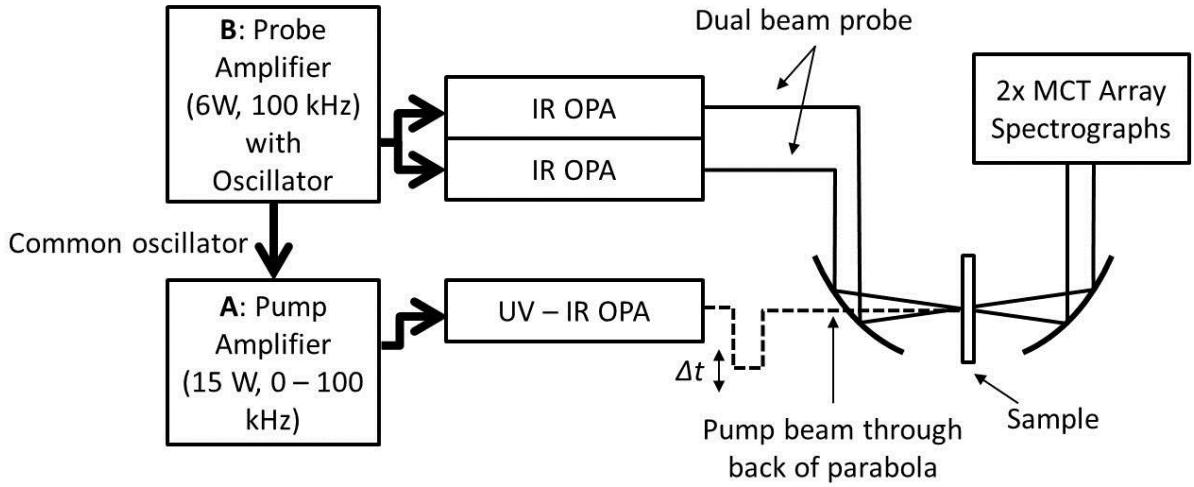

Figure 1. Schematic of dual-amplifier laser system, with OPA and experiment layout.

Typical experiments involve two mid-IR probe beams and a single UV-vis pump beam. The two probe beams exiting the OPAs are collimated, synchronised by a fixed optical delay and then focussed (to typically 50 – 75 μm diameter) by a gold parabolic mirror (7.5 cm focal length) on to a sample. The pump beam is similarly collimated, travels over a computer programmable 0 – 16 ns optical delay (1200 mm long, double pass) and then focussed (to typically 120 – 150 μm diameter) . The pump and probes beams are overlapped at the sample using a 50 μm diameter pinhole at the sample position. Care was taken to match probe beam spot-sizes to avoid any differences in their interaction with the pumped sample. Although our experience has been that the data from the two probe regions compare very well (e.g. data of fig. 4 is consistent with single broadband data from ref. 17, without correction), one should be cautious when comparing intensities of two probe regions.

After the sample, the two probe beams enter independently tunable homemade spectrographs and spectra are measured on two 128-element MCT detector arrays (IR Associates). The spectrum acquired by each MCT detector is integrated and digitised by an FPAS system (Infrared Systems Development Corporation, FPAS0144) to 16 bit precision. This 16 bit is essentially reduced to ~ 10 bit dynamic range due to detector noise limitations (~ 36 counts noise on a maximum of 65536) discussed in the next section. This data is then transferred from the FPAS systems to high speed digital I/O cards (25 MHz, 32 channels, NI PXIe 6536) in an industrial PXIe based PC (NI PXIe-8135) and processed. To avoid lost shots due to large amounts of data accumulation, software buffering in LabVIEW (National Instruments) sends data through raw acquisition, data sorting (to combine spectra from multiple, synchronized FPAS systems) and processing stages (to generate difference spectra), using data queues in blocks of typically 100 shots of 256x16 bit channels. Pump on – off difference signal measurements are normalised and averaged over a number of pump shots, at which point the PC memory required becomes significantly reduced. Absorption difference spectra

are calculated as described previously[1, 16]. This 320 element detection and data acquisition system is currently limited to < 200,000 acquisitions (each of up to 320 element spectra) per second. This limit is currently dictated by the analogue to digital conversion and digital I/O transfer in terms of our electronics. However, the MCT detection is also near its limit in terms of detector response time of ~ 2 µs, ultimately limiting this type of system to < 400 kHz rates. Reference spectra of a small portion of the probe beams not passing through the samples can also be measured simultaneously on two further 32-element array spectrometers (acquired by another synchronised FPAS system in the above arrangement, FPAS6416), to remove spectral and energy instabilities of the probe beams. However, because of the excellent stability of the IR outputs (as discussed later), no referencing or background fitting has been applied in the measurements shown here. Therefore only 256 elements are typically acquired.

Relative pump – probe timing control between the two Yb:KGW amplifiers is programmable from < 100 fs to 10 µs, using a combination of oscillator roundtrip timing to achieve steps of 12 ns and translation stage optical delay of the pump similar to our previous work[1]. Here, we opted for optical delay of the OPA output, whereas previously optical delay of the pump amplifier seed beam was used. The advantage of optically delaying the seed beam rather than the OPA output is that pump beam pointing at the sample is very reliable over varying optical delays, as the amplifier output pointing is defined by the regenerative amplifier cavity. There are however potentially serious consequences of a misaligned seed beam along a very long (> 12 ns) moving translation stage, such as optical damage in the amplifier and pulse duration variation from pointing changes in the seed stretcher, which in turn affects OPA performance.

Demonstration

A significant advance of the present laser system is the excellent stability of the Yb-based amplifier output over more conventional Ti:S systems. In high repetition rate pump – probe measurements, a critical parameter is the shot-to-shot stability of the mid-IR probe laser, which defines the noise limits of an IR absorption difference (pump on – pump off) measurement. While quantifying shot-to-shot intensity fluctuations in the present system over 1000 shots, we find the detection system to be the limiting factor, not the laser. Without laser light, we observe ~ 36 detector counts standard deviation (S.D.) from the detector system, whilst with laser on, we observed a small increase to 43 counts (on 44000 total, < 0.1 % S.D.), suggesting that the detector noise is dominant and the laser noise is on the order of < 0.06 % S.D., as shown in fig. 2. Previous measurements on our laboratory's Ti:S systems have shown typical shot-to-shot noise on the order of 5 to 10 times higher than this[16], still close to the detector limit, but significantly higher. This would suggest that with the present system, referencing laser noise with a second detection system would in fact increase the noise of the overall system, rather than reduce it. Difference measurements presented throughout this paper have not been referenced. In difference measurements, the noise limits are dependent on the pump rate (effectively the rate at which the experiment is cycled). In an acquisition time of 0.1 seconds, pumping at 50 kHz and probing at 100 kHz, we observe changes in optical density (Δ OD) limits of ~ 10^{-5}.

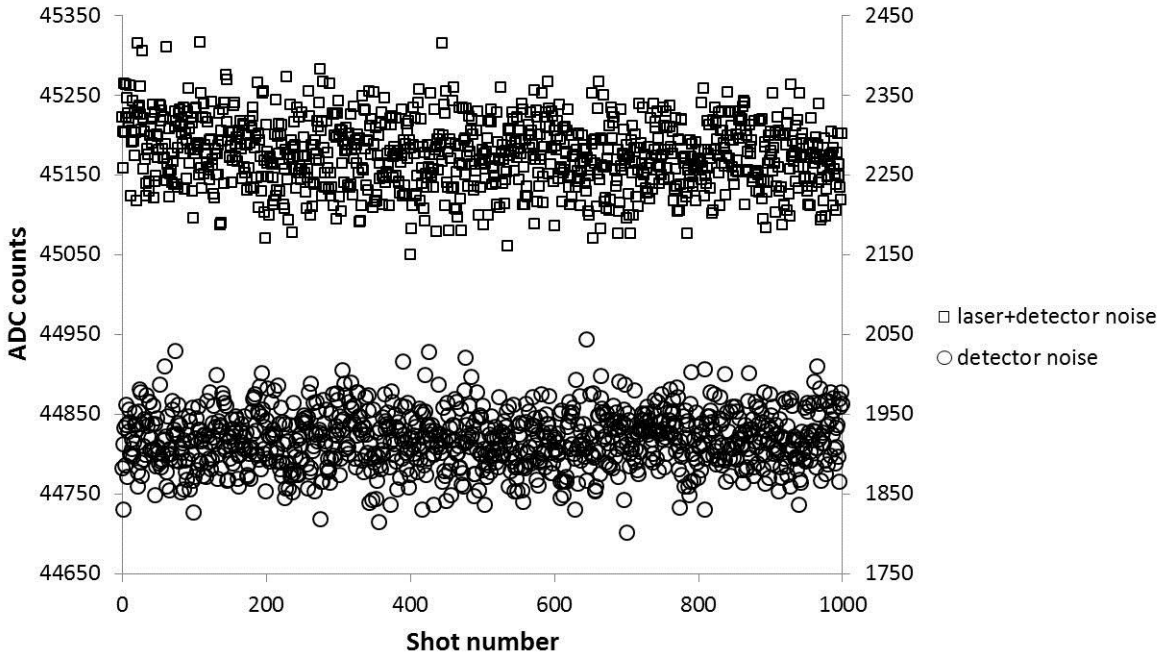

Figure 2. Laser noise comparison with detector noise over 1000 probe shots (0.01 seconds acquisition). Left scale is the intensity of the detector output with the laser on (squares). Right scale is the intensity of the detector output without the laser (circles).

Data acquisition times are dependent on the pump repetition rate of the experiment. To achieve sensitivity of Δ OD < 10^{-5}, at 50 kHz pump repetition rate (e.g. fig. 4), a single spectrum can be acquired in less than a second. An experiment of 1 kHz pump repetition rate (e.g. fig 6) requires several seconds to achieve the same sensitivity, although for each measurement (a single pump – 1st probe pulse time delay), 100 spectra are collected across 0 – 1 ms time delay. The lowest pump repetition rate experiments demonstrated in this work, 3 Hz, require several minutes to make a single measurement, which comprises of 33333 spectra across 0 – 333 ms. However, as can be seen in the data of fig. 7, noise levels in these low repetition rate experiments were limited to Δ OD > 10^{-4}.

Example mid-IR probe spectra from the Yb:YGW driven OPAs are shown in fig. 3, with the dual-bandwidth capability demonstrated in TRIR spectra of fig. 4. The TRIR spectra of figure 4 show IR spectral changes following 70 nJ, 400 nm excitation of coumarin 153 laser dye in deuterated acetonitrile (pathlength 100 μm, 0.4 OD at 400 nm). Although narrower than the broadband IR output of shorter pulsed Ti:S laser systems[16], there is clearly a usable spectrum extending beyond 200 cm^{-1} (note that the low wavenumber spectra of fig. 4 are limited by spectrograph bandwidth, not laser bandwidth). With the dual spectral region probing described above, the total bandwidth can be > 400 cm^{-1}. The two regions in fig. 4 were collected simultaneously and compare well with ref. 17.

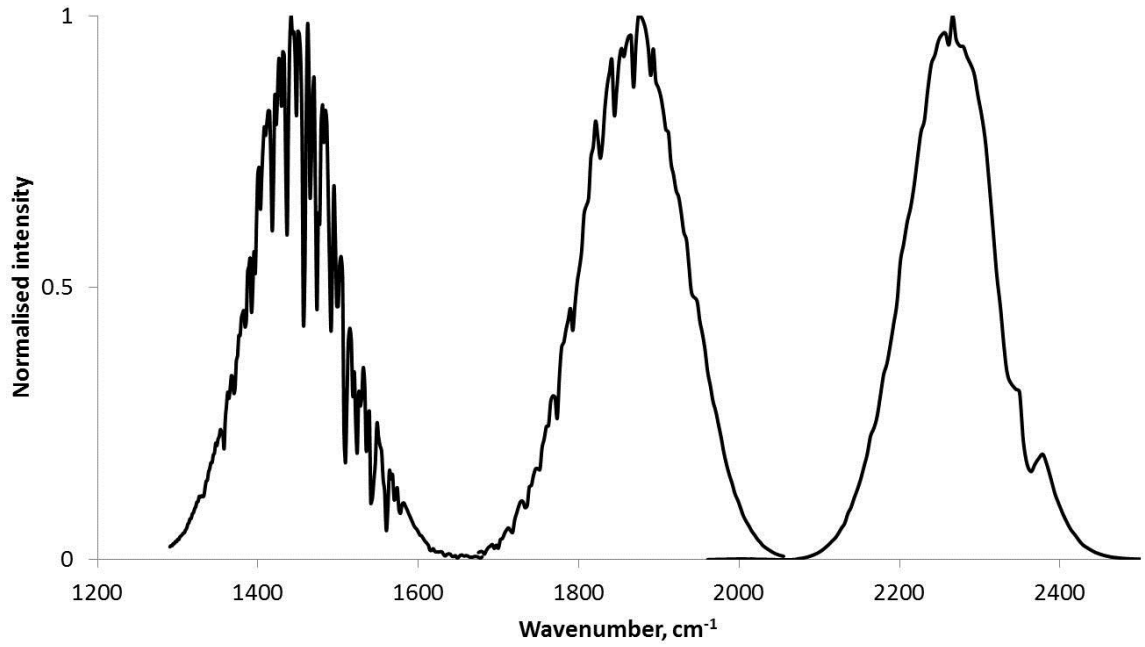

Figure 3. Three examples of a single OPA probe output spectrum, demonstrating > 200 cm^{-1} usable bandwidth across the mid-IR region. The fine structure in the spectra stem from water vapour and CO_2, normally removed by purging with dry nitrogen.

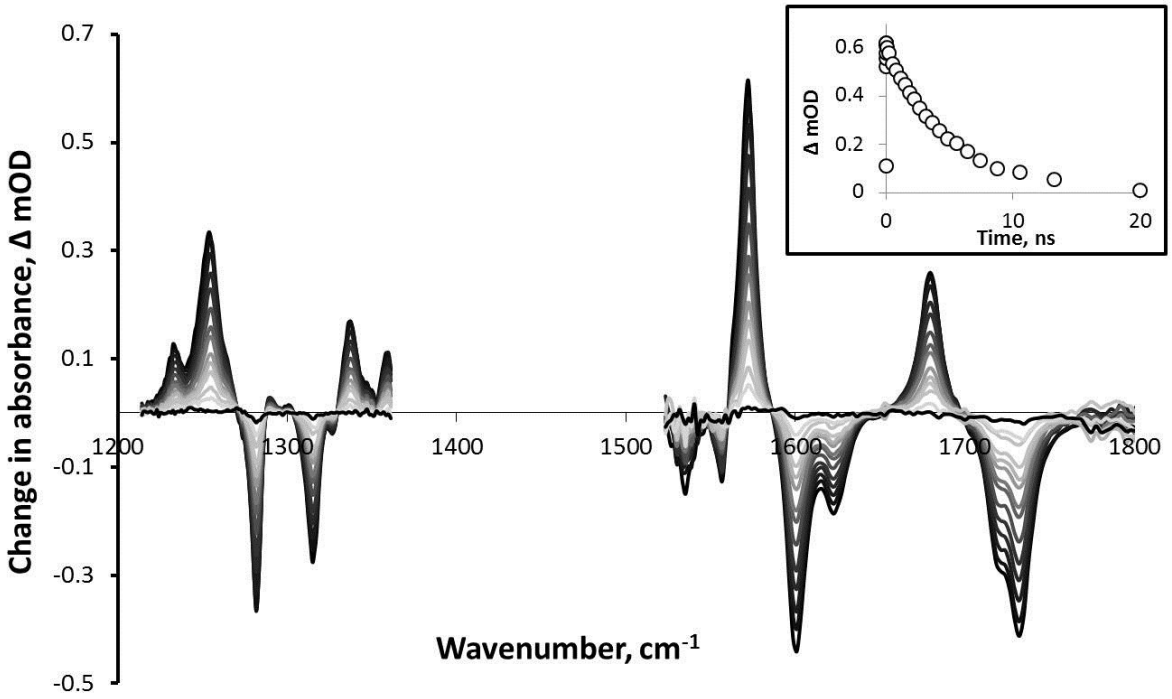

Figure 4. Time-resolved IR spectra of coumarin 153 laser dye, at 50 kHz pumping, 100 kHz probing, showing simultaneous measurement of two probe regions, with two probe OPA outputs. The inset shows kinetics of excited state decay over 10 ns, based on peak height changes at 1572 cm^{-1}.

To quantify the temporal response of the system, a Kerr effect measurement was performed in a 0.5 mm piece of CaF_2, using 310 nm pump pulses (300 nJ) and probing at 5 μm. Pump and probe beam relative polarization was set to 45°. After the sample, the probe intensity was minimised to ~ 10% by passing through a polarizer. By rotating the polarisation of the UV beam from +45 to -45, the transient change in transmission of the IR light through the polariser could be made positive or negative. Fig. 5 shows this temporal response, with a 200 fs full width half maximum. The relative UV – IR group velocity mismatch in the CaF_2 could

contribute as much as 87 fs, so the temporal response is < 200 fs. As a secondary instrument response measurement, the formation of the $W(CO)_6$ bleach at 1976 cm^{-1} upon photolysis (see below and ref. 1) was measured in acetonitrile. Despite convolution of this rise with coherence effects at negative time and sample response, the rise time was still measured to be sub-picosecond, ~ 500 fs. Given an instrument response of < 200 fs, the fundamental 1030 nm pump and probe amplifier pulse durations (260 and 180 fs, respectively) are shortened slightly through the OPA conversion processes. We expect that the temporal width of the pump pulse is the limiting factor, considering longer duration of its fundamental output compared with duration of the probe fundamental. Pump and probe pulse durations at the OPA outputs are estimated to be ≤ 150 fs.

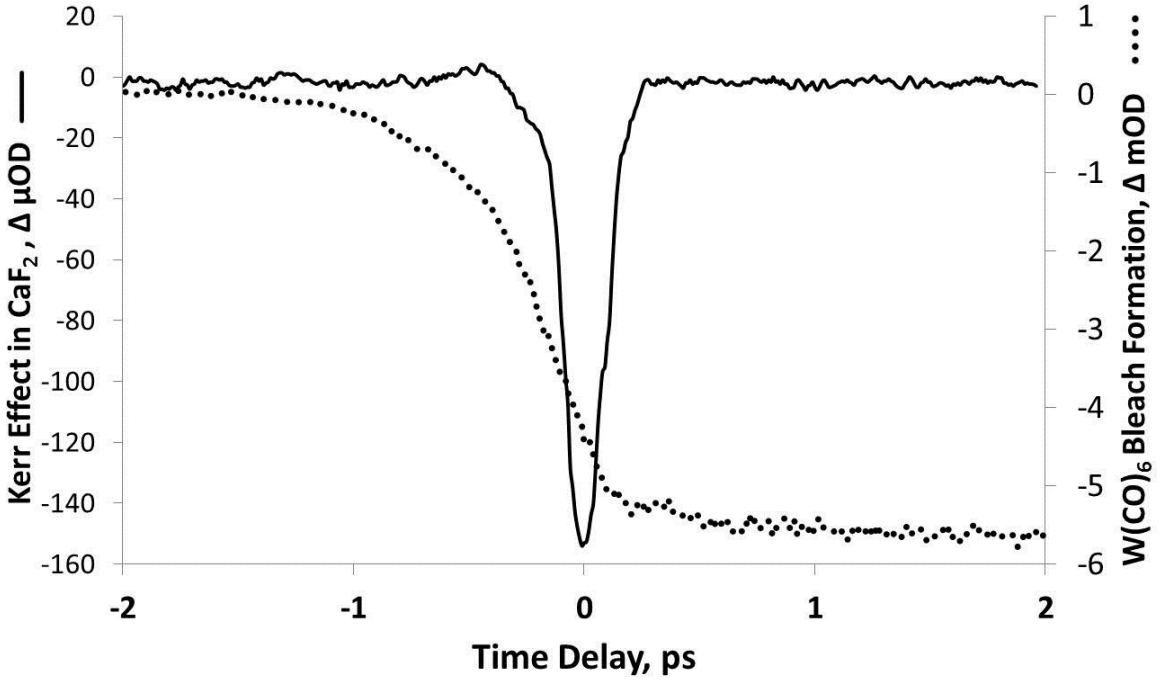

Figure 5. Temporal response of the pump – probe pulses measured by Kerr effect in CaF_2 (solid line) and rise time of the main 1976 cm^{-1} bleach during photolysis of $W(CO)_6$ in acetonitrile (dotted line).

In our previous TRMPS work, we demonstrated time-resolved measurements on the photodissociation of $W(CO)_6$ and the subsequent solvent association (< 1 ps), cooling (< 1 ns) and diffusion-limited exchange of trace contamination water with solvent (> 100 μs). We achieve significantly improved results here, with the several orders of magnitude dynamics shown in fig. 6. The TRIR measurements of $W(CO)_6$ in heptane shown in fig. 6 were taken using 0.5 μJ, 350 nm pumping of a sample, 0.4 OD at 1984 cm^{-1} in a 100 μm path-length cell. Typical bleach intensities at 1984 cm^{-1}, due to the loss of the $W(CO)_6$ parent molecule, were 2 mOD. The 100 kHz system probes changes every 10 μs, rather than every 100 μs in the 10 kHz probe system described previously. Additionally, the easily adjustable pump repetition rate and improved stability of the laser system allows simple extension of these measurements to longer times (beyond milliseconds), and allows the optimisation of pump rate to the sample refresh rate, to avoid repumping photo-products. In this manner, high pump repetition rates are used for samples with rapid recovery (see example of fig. 4), while low repetition rates are better for slow- or non-recovering samples (see example of fig. 7).

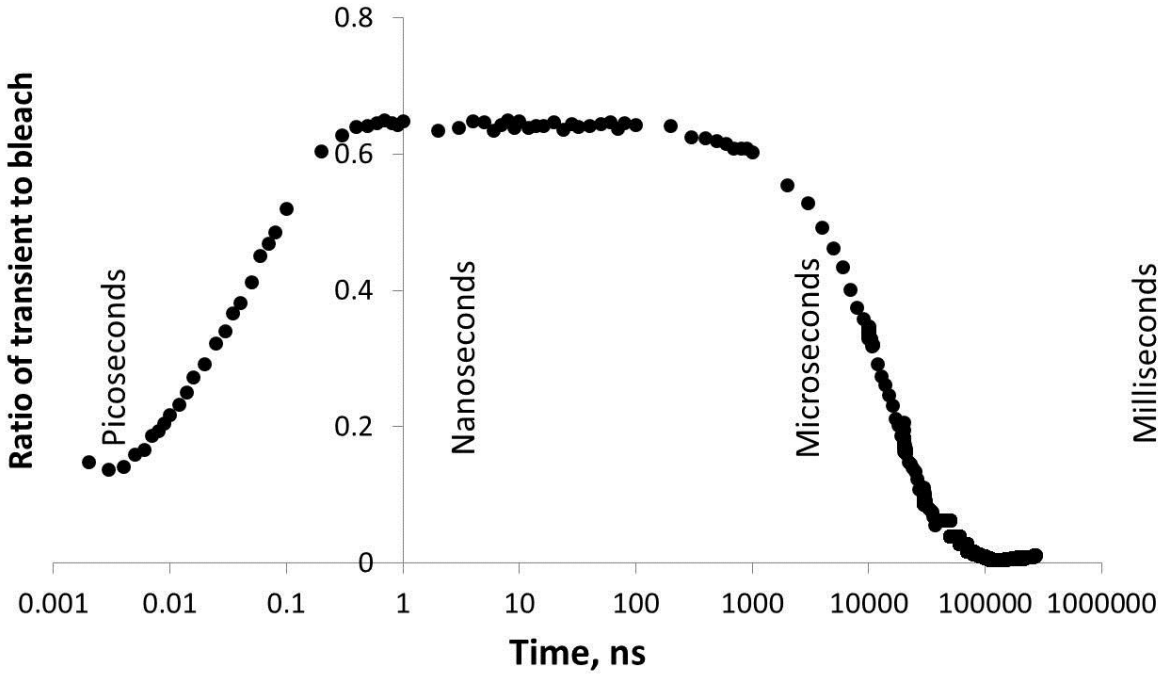

Figure 6. Kinetics of $W(CO)_6$ photo-dissociation in heptane solution, shown as the ratio of $W(CO)_5$(heptane) adduct formation (1956 cm^{-1}) to $W(CO)_6$ loss (1984 cm^{-1}) on a logarithmic time-scale. Sub-nanosecond kinetics show early time formation and cooling of the heptane adduct formed following the loss of CO. Beyond 1 μs, heptane is replaced by water at a diffusion-limited rate to form $W(CO)_5$(water), resulting in the loss of $W(CO)_5$(heptane).

To explore the limit of slow sample recovery, we performed 3 Hz pumping experiments on a spiro-oxazine. Ultrafast to near-seconds dynamics were observed, whilst still obtaining ΔOD ~ 10^{-4} fidelity in the measurements. Spiro-oxazines are photochromic molecules which follow a ring-opening reaction when excited by UV light. The ring-opening results in a dramatic colour change. Here, 5-Chloro-1,3-dihydro-1,3,3-trimethylspiro[2*H*-indole-2,3′-(3*H*)naphth[2,1-*b*](1,4)oxazine] in deuterated acetonitrile was observed to change from colourless to blue/purple. The typical recovery time of the colourless form was approximately a second, to the naked eye. Fig. 7 shows the TRIR spectra recorded, with 350 nm pumping

(few hundred nanojoules energy per pulse) of a 100 μm path-length, optical density 0.5 at 350 nm. Similar spectra of a spiro-pyran ring-opening reaction by Rini et al.[18], exhibit strong spectral bleaches in the first few picoseconds at 1485 and ~ 1600 cm^{-1} which recover as most of the excited S_1-state ring-closed molecules return to the S_0 ground-state, with the photochemical formation of the ring-open form having a quantum yield of ~ 0.1. Recovery to the ring-closed form was not observed over a 20 ms timescale. In the current setup, it was not possible to see the (>> 100 ms) recovery of the system, which would require < 1 Hz pumping. The 3 Hz lower-limit was due to the vast amount of data produced by each pump shot (33333 spectra!). To extend the method from ultrafast to quasi-continuous-wave probing, probe data can in future be compressed towards longer times into manageable sizes, without losing significant kinetic information.

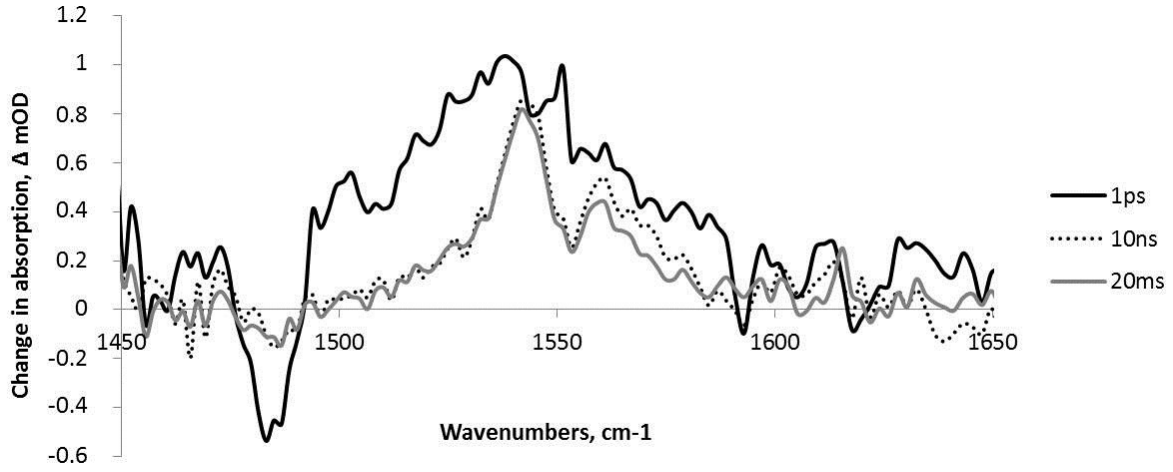

Figure 7. Time-resolved multiple probe IR spectra of spiro-oxazine, with 3 Hz pumping, 100 kHz probing.

Data Analysis

As many transient absorption experiments are limited by sample recovery to pump rates of ≤ 5 kHz, scaling of data rate can typically only be applied to the probe. In the TRMPS method of recording a transient absorption spectrum, for every pump laser shot, there are *n* probe laser shots. The femtosecond to microsecond dynamics are observed on the first probe pulse and the microsecond to millisecond dynamics are observed on subsequent probe pulses. It is important to note that for every combination of pump pulse delay and intensity, pump – probe overlap and sample uniformity used, data is continuously recorded for all subsequent probe pulses. As mentioned in our previous work[1], the TRMPS method provides information on a variety of artefacts and noise sources, not observed in pump on – off difference measurement recorded with probe repetition rate of *k* and pump rate *k*/2. In the present 100 kHz system, we have 10x the probe pulses per experiment than our previous system and these noise patterns and artefacts are increased in clarity. Here we present a summary of observations and potential enhancements available from this type of measurement.

There are several common sources of error in high repetition rate pump – probe measurements which can be separated into general noise and measurement artefacts stemming from the manner of data acquisition. In terms of signal noise, these are typically caused by (*i*) sample inhomogeneity during raster scanning and (*ii*) noise from laser instability, such as pump pointing and intensity fluctuations. Artefacts can arise from sources such as (*iii*) insufficient sample flow rates (or sample movement), meaning that the sample has not been completely removed from the pump – probe interaction region before repumping, causing photo-products to interfere with measurements, or (*iv*) the flow itself is observed as a dynamic change in the system and changes are still occurring during the "pump off" measurement. Other artefacts can be caused by (*v*) pump pointing or divergence changes while scanning optical delays over, potentially, metres of travel.

Artefacts caused by flow rate ((*iii*) and (*iv*)) are easily observed in a TRMPS measurement. Under continuous flow conditions, long timescale probing of the sample tracks the movement of the sample out of the pump focus region, typically on a timescale of 100 μs to several milliseconds, as long as the sample changes show signals on these timescales (as shown in our previous work). Any signal changes caused by variation in flow rate can be verified by changing this rate, to avoid confusion with real sample changes.

The other errors mentioned above ((*i*), (*ii*) and (*v*)) can also be characterised in TRMPS measurements, as they reveal themselves through repeating noise patterns in the multiple-probe measurements. Each pump – probe measurement includes uncertainty due to variation in the sample and pump laser conditions. The later probe pulses contain a degree of the same noise, while the dependence of the real sample kinetics on the mechanical and electrical delays is insignificant for these probe measurements. For example, when measuring kinetics over the first 10 ns, the second probe pulse measures changes over 10 – 10.01 μs and the third over 20 – 20.01 μs. The variations of signal within the second, third and subsequent probe measurements therefore only inform on noise and system artefacts rather than kinetics of these earlier time changes.

The noise patterns accessible through the TRMPS method are clearly shown in the kinetic profiles shown in fig. 8a, where an intentional misalignment of the delay line is portrayed as a repeating pattern in $W(CO)_6$ photo-dissociation data (see above). Root mean square, RMS, of the spectrum is taken as a measure of general pump-induced changes. The pattern shows dropping signal intensity in the 1 – 10 ns region and likewise in the 50.001 – 50.010 μs region and so on, due to the delay line misalignment. A principal component analysis (PCA) of this data (LabVIEW) shows the dominant component (dotted line in fig. 8a), by two orders of magnitude over any other component, to be the delay line artefact. Using this component

to correct the data removes this distortion (fig. 8b and 8c). Correction is made by simply dividing the data by the normalised dominant component.

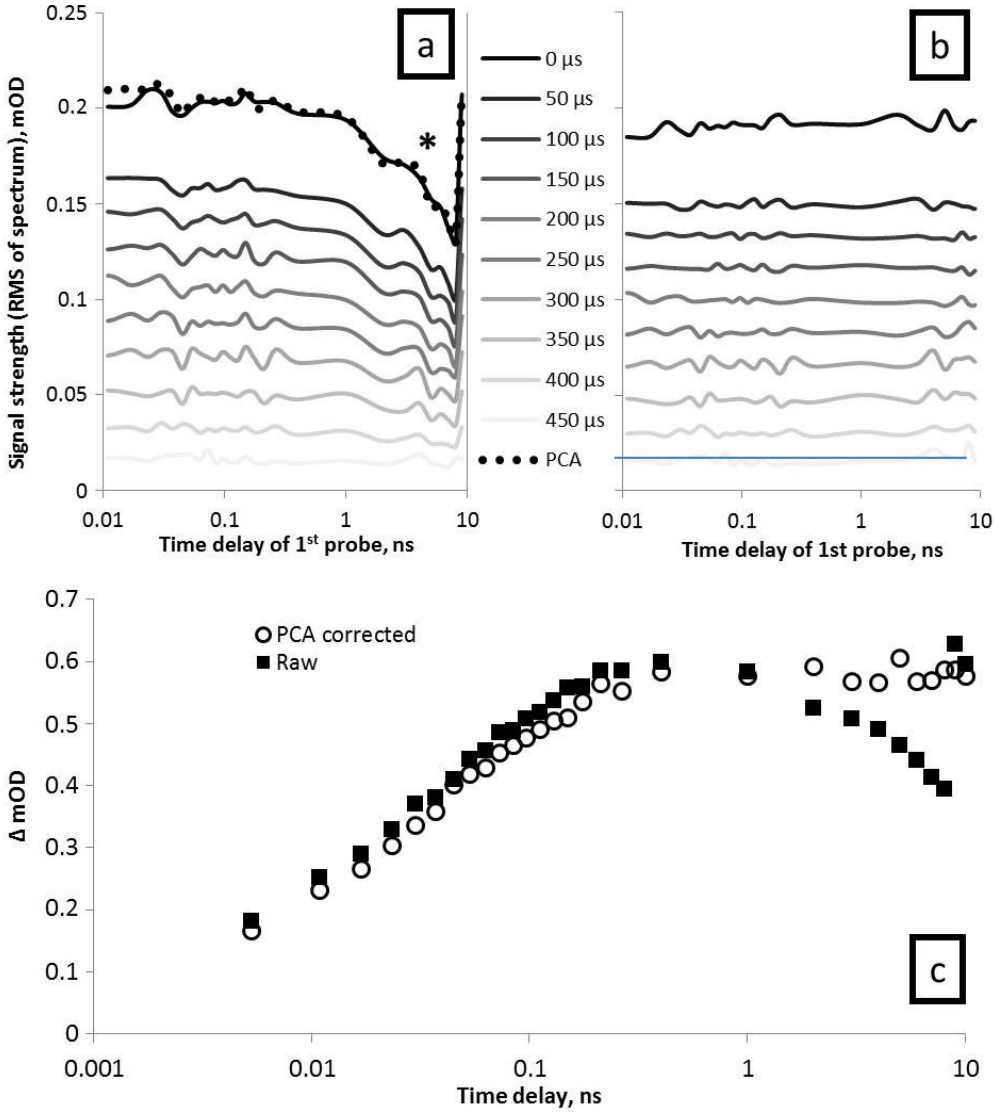

Figure 8. PCA of repeated probing for artefact and noise removal. (a) and (b) show repeating noise patterns within subsequent probe measurements, with only every 5th probe shown for clarity, with (a) being the acquired data and (b) being the PCA corrected data. The asterisk highlights an intentionally induced artefact caused by poor alignment of the optical delay line. The signal intensity is represented as the RMS of the spectra in (a) and (b). (c) is

the kinetic profile of the $W(CO)_5$(heptane) adduct signal at 1956 cm^{-1} during the initial vibrational cooling, showing removal of the delay line scanning artefact.

As well as removal of such artefacts, pump energy and pump - probe overlap fluctuations can also be removed by this PCA method. For example, if a pump pulse shows half energy on one measurement, subsequent probe spectra will all show this halving of the absorption change in intensity, something which would be clearly identifiable by PCA.

Summary

We have described a new dual-amplifier laser for TRIR and IR TRMPS. The Yb:KGW laser system provides improved efficiency and higher signal to noise compared to conventional Ti:S systems. The impact of the limitations in pulse duration and spectral bandwidth of this Yb:KGW system have been explored and demonstrated as adequate for practical measurements, with temporal response of < 200 fs recorded and dual probe capability (> 400 cm^{-1} total) minimising the latter limitation. TRIR spectra, with variable pump repetition rate, between 3 Hz and 50 kHz, over many orders of magnitude in time have been demonstrated, showing 13 orders of time are accessible with the present system, accessing femtosecond to second molecular structure dynamics. Finally, we have shown how the multiple-probing technique allows new methods for noise and artefact removal. Repeated probing of the sample generates repeated patterns of correlated noise and artefacts in the measurements, which can be evaluated by PCA.

Acknowledgments

We would like to acknowledge financial support from BBSRC, under grant Alert 13 BB/L014335/1, and STFC Central Laser Facility. We are grateful to Vytautas Sinkevičius of Light Conversion Ltd. for collaboration in development of IR OPA bandwidth. Sergey Laptenok is acknowledged for feedback on initial test results on the system.

References

1. G. M. Greetham, D. Sole, I. P. Clark, A. W. Parker, M. R. Pollard, M. Towrie, *Rev. Sci. Instrum*, **83**, 103107, (2012).

2. C. J. Wood, M. Cheng, C. A. Clark, R. Horvath, I. P. Clark, M. L. Hamilton, M. Towrie, M. W. George, L. C. Sun, X. C. Yang and E. A. Gibson, *J. Phys. Chem. C*, **118**, 16536, (2014).

3. H. van der Salm, M. G. Fraser, R. Horvath, J. O. Turner, G. M. Greetham, I. P. Clark, M. Towrie, N. T. Lucas, M. W. George and K. C. Gordon, *Inorganic Chem*, **53**, 13049, (2014).

4. A. Lukacs, A. Haigney, R. Brust, K. Addison, M. Towrie, G. M. Greetham, G. A. Jones, A. Miyawaki, P. J. Tonge and S. R. Meech, *J. Phys. Chem. B*, **117**, 11954, (2013).

5. R. Brust, A. Lukacs, A. Haigney, K. Addison, A. Gil, M. Towrie, I. P. Clark, G. M. Greetham, P. J. Tonge and S. R. Meech, *J. Am. Chem. Soc*, **135**, 16168, (2013).

6. H. J. Russell, S. J. O. Hardman, D. J. Heyes, M. A. Hough, G. M. Greetham, M. Towrie, S. Hay and N. S. Scrutton, *FEBS J*, **280**, 6070, (2013).

7. A. F. E. Hauck, S. J. O. Hardman, R. J. Kutta, G. M. Greetham, D. J. Heyes and N. S. Scrutton, *J. Biological Chem*, **289**, 17747, (2014).

8. S. J. O. Hardman, A. F. E. Hauck, I. P. Clark, D. J. Heyes and N. S. Scrutton, *Biophysical J*, **107**, 2195, (2014).

9. D. J. Heyes, S. J. O. Hardman, T. M. Hedison, R. Hoeven, G. M. Greetham, M. Towrie and N. S. Scrutton, *Angewandte Chemie-International Ed*, **54**, 1512, (2015).

10. S. P. Laptenok, A. Lukacs, A. Gil, R. Brust, I. V. Sazanovich, G. M. Greetham, P. J. Tonge and S. R. Meech, *Angewandte Chemie*, **accepted for publication**, (2015).

11. H. Liu, J. Nees, G. Mourou, S. Biswal, G. J. Spuhler, U. Keller and N. V. Kuleshov, *Optics Comms*, **203**, 315, (2002).

12. C. Schnedermann, M. Liebel, and P. Kukura, *JACS*, **137**, 2886, (2015).

13. R. Antipenkov, A. Varanavicius, A. Zaukevicius and A. P. Piskarskas, *Optics Express*, **19**, 3519, (2011).

14. M. Bradler, C. Homann and E. Riedle, *Appl. Phys. B*, **113**, 19, (2013).

15. J. Bredenbeck, J. Helbing, and P. Hamm, *Rev. Sci. Instrum*. **75**, 4462, (2004).

16. G. M. Greetham, P. Burgos, Q. A. Cao, I. P. Clark, P. S. Codd, R. C. Farrow, M. W. George, M. Kogimtzis, P. Matousek, A. W. Parker, M. R. Pollard, D. A. Robinson, Z. J. Xin and M. Towrie, *Appl. Spec*, **64**, 1311, (2010).

17. M. W. D. Hanson-Heine, A. Wriglesworth, M. Uroos, J. A. Calladine, T. S. Murphy, M. Hamilton, I. P. Clark, M. Towrie, J. Dowden, N. A. Besley, and M. W. George, *J. Chem. Phys*, **142**, 154119, (2015).

18. M. Rini, A. K. Holm, E. T. J. Nibbering and H. Fidder, *JACS*, **125**, 3028, (2003).

Figure Captions

Figure 1. Schematic of dual-amplifier laser system, with OPA and experiment layout.

Figure 2. Laser noise comparison with detector noise over 1000 probe shots (0.01 seconds acquisition). Left scale is the intensity of the detector output with the laser on (squares). Right scale is the intensity of the detector output without the laser (circles).

Figure 3. Three examples of a single OPA probe output spectrum, demonstrating > 200 cm^{-1} usable bandwidth across the mid-IR region. The fine structure in the spectra stem from water vapour and CO_2, normally removed by purging with dry nitrogen.

Figure 4. Time-resolved IR spectra of coumarin 153 laser dye, at 50 kHz pumping, 100 kHz probing, showing simultaneous measurement of two probe regions, with two probe OPA outputs. The inset shows kinetics of excited state decay over 10 ns, based on peak height changes at 1572 cm^{-1}.

Figure 5. Temporal response of the pump – probe pulses measured by Kerr effect in CaF_2 (solid line) and rise time of the main 1976 cm^{-1} bleach during photolysis of $W(CO)_6$ in acetonitrile (dotted line).

Figure 6. Kinetics of $W(CO)_6$ photo-dissociation in heptane solution, shown as the ratio of $W(CO)_5$(heptane) adduct formation (1956 cm^{-1}) to $W(CO)_6$ loss (1984 cm^{-1}) on a logarithmic time-scale. Sub-nanosecond kinetics show early time formation and cooling of the heptane adduct formed following the loss of CO. Beyond 1 μs, heptane is replaced by water at a diffusion-limited rate to form $W(CO)_5$(water), resulting in the loss of $W(CO)_5$(heptane).

Figure 7. Time-resolved multiple probe IR spectra of spiro-oxazine, with 3 Hz pumping, 100 kHz probing.

Figure 8. PCA of repeated probing for artefact and noise removal. (a) and (b) show repeating noise patterns within subsequent probe measurements, with only every 5^{th} probe shown for clarity, with (a) being the acquired data and (b) being the PCA corrected data. The asterisk highlights an intentionally induced artefact caused by poor alignment of the optical delay line. The signal intensity is represented as the RMS of the spectra in (a) and (b). (c) is the kinetic profile of the $W(CO)_5$(heptane) adduct signal at 1956 cm^{-1} during the initial vibrational cooling, showing removal of the delay line scanning artefact.